Mg-ion diffusion on the surface of $Ti_3C_2S_2$ MXene

Konstantina A. Papadopoulou, Alexander Chroneos and Stavros-Richard G. Christopoulos

Original citation:
Papadopoulou, K.A., Chroneos, A. and Christopoulos, S.R.G., 2022. Mg-ion diffusion on the surface of Ti3C2S2 MXene. *Journal of Physics and Chemistry of Solids*, 110713. https://doi.org/10.1016/j.jpcs.2022.110713

DOI 10.1016/j.jpcs.2022.110713
ISSN 0022-3697

Publisher: Elsevier

Journal of Physics and Chemistry of Solids 166 (2022) 110713

Contents lists available at ScienceDirect

Journal of Physics and Chemistry of Solids

journal homepage: www.elsevier.com/locate/jpcs

Mg-ion diffusion on the surface of $Ti_3C_2S_2$ MXene

Konstantina A. Papadopoulou [a], Alexander Chroneos [b,c], Stavros-Richard G. Christopoulos [a,*]

[a] Faculty of Engineering, Environment and Computing, Coventry University, Priory Street, Coventry, CV1 5FB, United Kingdom
[b] Department of Electrical and Computer Engineering, University of Thessaly, 38221, Volos, Greece
[c] Department of Materials, Imperial College London, London, SW7 2BP, UK

ARTICLE INFO

Keywords:
MXenes
Diffusion barrier
Transition state
Bond valence sum
Conductive pathways
Mg-ion diffusion
Adsorption

ABSTRACT

Obtaining the structure of the $Ti_3C_2S_2$ MXene using Density Functional Theory, we study here for the first time the adsorption and diffusion of an Mg ion on the surface of the MXene. We find a very strong adsorption and the lowest energy barrier for Mg diffusion in Ti_3C_2-based materials reported so far. This value, equal to 0.049 eV, is comparable to the one for the diffusion of a Li ion on the surface of the $Ti_3C_2Cl_2$ MXene reported in previous studies, which was equal to 0.03 eV. The $Ti_3C_2S_2$ MXene could, therefore, potentially present as the best option for an anode electrode in Mg-ion batteries, while offering a safer, lower cost alternative to Li-ion batteries.

1. Introduction

Useful in electric vehicles as well as portable electronic devices like mobile phones and laptops, Li-ion batteries (LIB) have been accepted as the most common power source [1]. LIB advantages lie with their light weight, long cycle durability, and higher energy density than its predecessors [2]. In addition, Li-ions have small atomic radius, thus exhibiting high diffusion coefficient [3].

Despite the aforementioned factors that make LIB widely used, there are still problems that arise with their continuous usage. For example, LIB have not yet provided a solution for large-scale applications [4], like sustaining a clean power grid [5]. The main disadvantage currently is the limited lithium reserves [1]. In addition, there is a variety of safety issues when it comes to Li-metal anode electrodes [6], especially the forming of lithium dendrites. For these reasons, attention has been shifted in recent years to technologies beyond the use of Li.

Batteries based on multivalent atoms are the most studied ones due to their higher volumetric capacity [6]. In particular, Mg-metal anodes have garnered interest due to the thermodynamic properties of magnesium [7]. Mg-ion batteries (MIB) are dendrite-free, thus safer than LIB, lower cost since Mg reserves can be found in abundance [6], and, because Mg ions are divalent, they offer higher energy density [8]. The use of MIB, however, does not come without its own obstacles.

A major setback is the fact that the intercalation of Mg-ions into 3D compounds lacks understanding [9]. For that reason, MXenes are being studied as energy storage materials since they are versatile and their structure allows for fast ion transport.

MXenes are a new family of 2D materials first produced by etching MAX phases [10]. The latter have the general formula $M_{n+1}AX_n$, ($n = 1$, 2, 3), [M an early transition metal (groups 3–7 in the periodic table), A an element belonging in the A-group of the periodic table, and X is carbon (C) or nitrogen (N) [4,11–13]] and were soaked into acid, thus destroying the bonds between T and A. The result was 2D flakes, the MXenes, with the general formula $M_{n+1}X_nT_x$, ($n = 1$, 2, 3), where T stands for a surface termination atom [14].

In 2014, Xie et al. [15] theoretically studied MXene nanosheets as anode materials for non-lithium-ion batteries. They found that OH-terminated Ti_2C is not a desirable material since it exhibits poor Mg-ion adsorption and a migration barrier energy for the Mg ion equal to 0.425 eV, a value close to that for a Li ion (0.503 eV [16]). Moreover, they showed that the Mg ion in the $Ti_3C_2O_2$ MXene exhibits strong adsorption but a migration barrier energy larger than 0.5 eV, thus rendering the material unsuitable for anode electrode.

In 2018, Xu et al. [17] using Density Functional Theory (DFT) simulations reported that the Mg ion cannot be easily adsorbed by OH and F terminations in Ti_3C_2. In addition, the migration barrier energy for the Mg ion in the Ti_3C_2O MXene was found larger than 0.8 eV (see Fig. 3 of Ref. 17).

In 2020, Kaland et al. [18] using both DFT simulations and experiment found that the Mg ion does not adsorb on the surface of single-layer $Ti_3C_2(OH)_2$ and single-layer $Ti_3C_2F_2$, exhibiting positive adsorption energies in both cases. Moreover, they calculated the Mg migration

* Corresponding author.
E-mail address: ac0966@coventry.ac.uk (S.-R.G. Christopoulos).

https://doi.org/10.1016/j.jpcs.2022.110713
Received 28 January 2022; Received in revised form 22 March 2022; Accepted 28 March 2022
Available online 6 April 2022

barrier energy in single-layer $Ti_3C_2O_2$ at 0.808 eV.

Also in 2020, Zhu et al. [2] examined two cases for interlayer spacing in $Ti_3C_2O_2$. They found migration barriers for an Mg ion equal to 0.57 eV and 0.53 eV when the interlayer spacing increased from 1.4 nm to 1.8 nm respectively. These results were validated through DFT.

Finally, in 2021, Chaney et al. [19] using DFT found that the Mg ion's migration barrier in Ti_2CS_2 was in the range of 0.45–0.52 eV.

In the present paper, we study the adsorption and mobility of an Mg ion on the surface of the $Ti_3C_2S_2$ MXene, a material never before examined. We show that $Ti_3C_2S_2$ exhibits lower migration barrier for Mg than all the Ti_3C_2-based materials studied so far, a fact that makes it the most promising material for anode electrode in MIB batteries. The reason for choosing Ti_3C_2 as a substrate, is the fact that, up to now, this particular MXene remains the most conductive one [20,21].

2. Computational methods

For the bulk structure of Ti_3C_2 with no termination atoms, we used an initial cell suggested in both experimental and theoretical analysis [10,22]. We performed electronic structure calculations within the framework of DFT using the CASTEP package [23–27]. DFT uses pseudopotentials [28] to describe the electron-ion interactions [29]. The exchange-correlation interactions between electrons were described by the generalized gradient approximation (GGA) method.

A vacuum space of 30 Å [30] was introduced between adjacent layers to minimize the mirror interactions between the upper and bottom layers. A plane wave cut-off energy $E_{cut} = 650$ eV and a k-point spacing of $6 \times 6 \times 1$ was used in order to converge the overall energy per formula unit to 10^{-5} eV.

The structures were fully optimized using Broyden - Fletcher - Goldfarb - Shanno (BFGS) geometry optimization method [27,31]. All structures were relaxed until the residual forces on the atoms declined to less than 0.01 eV $\times$ Å^{-1}.

After obtaining the $Ti_3C_2S_2$ structure, we applied DFT anew inserting an Mg ion on the surface of the structure, and at a distance from the S atoms equal to the bond length R_0 between S and Mg. The bond length is defined as the distance between the nuclei of two bonded atoms [32].

To calculate the energy barrier for an Mg ion to diffuse on the surface of $Ti_3C_2S_2$ we worked as follows: First, we created a $2 \times 1 \times 1$ supercell of the structure. The initial position of the Mg ion, which is called reactant, was that predicted after the aforementioned DFT calculations, while the final position, which is called product, was the same position in the adjacent cell. We then applied a full linear and quadratic synchronous transit (LST/QST) transition state (TS) search algorithm in CASTEP [33]. The migration barrier height was calculated as the barrier from reactant, that is, as the energy difference between the maximum and initial energy step.

To visualize the diffusion pathways, we used the Bond Valence Sum (BVS) model [32,34–38] which is based on Pauling's electrostatic valence principle [39]. Papadopoulou et al. [40] showed that BVS replicates the DFT results, particularly for diffusion pathways, with good accuracy and great time efficiency, without needing the exact positions of the atoms.

For the calculation of the bond valence sums, we used the command line form of the softBV software [41] and the parameters available therein [42].

In practice, we created a $2 \times 2 \times 1$ supercell of $Ti_3C_2S_2$. We then placed a grid of Mg ions inside the structure. Valid sites for the Mg ion to sit were the locations where the total BVS was within ± 0.2 valence units of the natural oxidation number of Mg which is equal to $+2$.

Finally, for a single Mg ion adsorption, we calculated the adsorption energy E_{ads} using the following equation:

$$E_{ads} = E_{Ti_3C_2S_2-Mg} - E_{Ti_3C_2S_2} - E_{Reference} \quad (1)$$

where $E_{Reference}$ is the total energy of a Mg atom in the Mg metal bcc phase. The latter was calculated by taking a $2 \times 2 \times 1$ supercell of metal-Mg_2 and applying DFT, then dividing the final energy by the total number of atoms in the supercell.

The figures in this paper were produced using the VESTA software [43].

3. Results & discussion

In Fig. 1 we see the $2 \times 2 \times 1$ supercell for the resulted $Ti_3C_2S_2$–Mg MXene layer. The S atoms sit in the fcc positions, in agreement with previous studies [30,44,45]. We have defined the fcc positions as the sites on the MXene's surface that no other atoms exist underneath them, a schematic of which can be found in Fig. 2 of Ref. [30]. In addition, the Mg ions favour the sites on top of the middle-level Ti atoms (see Fig. 1), which we will denote from now on as Ti2. Other possible adsorption sites for the Mg ions were the fcc positions, the positions above a top level Ti atom, and the hcp sites, i.e., the positions above a bottom level Ti atom. All these configurations, however, were less stable, and are not discussed here.

The adsorption energy E_{ads} for a single Mg ion on the surface of the $Ti_3C_2S_2$ MXene as calculated using Eq. (1) is -1.75 eV.

After the TS search, we found that the TS Mg will sit at the fcc position, thus the Mg ion will follow the path Ti2 – fcc – Ti2. This movement of the Mg ion is shown in Fig. 2a. The contour map of the pathway using the BVS model as discussed in Section II is shown in Fig. 2b.

Finally, the energy barrier for diffusion of the Mg ion on the surface of the $Ti_3C_2S_2$ MXene monolayer is 0.049 eV.

The energetically most favourable positions for the Mg ion were found to be the sites directly above a Ti2 atom. These sites exhibit strong adsorption (-1.75 eV), stronger than the fcc positions (-1.52 eV)

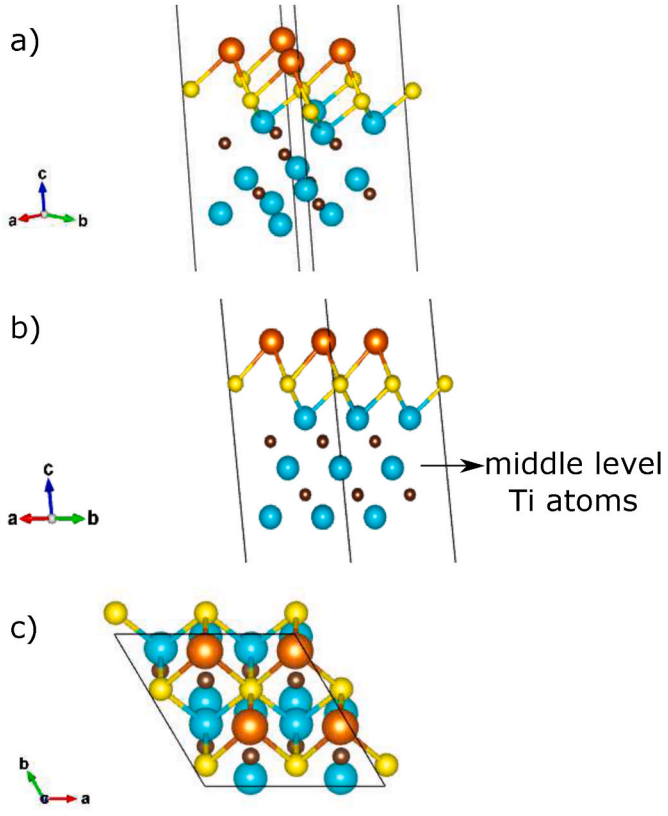

Fig. 1. The $2 \times 2 \times 1$ supercell for the $Ti_3C_2S_2$–Mg MXene layer after geometry optimization: a) 3D view, b) front view, c) top view. Blue spheres: Titanium atoms. Brown spheres: Carbon atoms. Yellow spheres: Sulfur atoms. Orange spheres: Magnesium ions. (For interpretation of the references to colour in this figure legend, the reader is referred to the Web version of this article.)

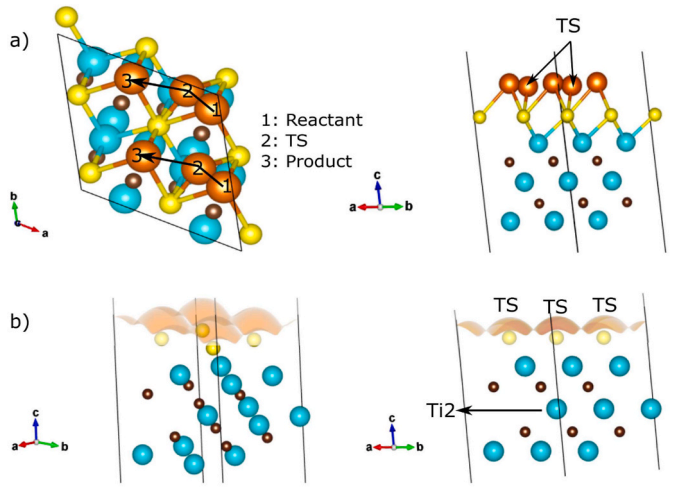

Fig. 2. a) Top view (left) and front view (right) of the 2 × 2 × 1 supercell for the $Ti_3C_2S_2$–Mg MXene layer, including the reactant, TS and product Mg-ion. The arrow indicates the direction of the diffusion. b) 3D view (left) and front view (right) of the 2 × 2 × 1 supercell for the $Ti_3C_2S_2$–Mg MXene layer including the contour map of the conductive pathways as calculated from the BVS model. Blue spheres: Titanium atoms. Brown spheres: Carbon atoms. Yellow spheres: Sulfur atoms. Orange spheres: Magnesium ions. (For interpretation of the references to colour in this figure legend, the reader is referred to the Web version of this article.)

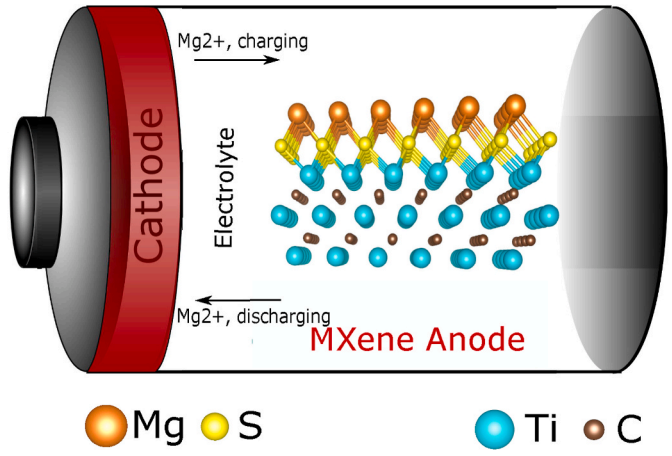

Fig. 3. The inner workings of a MIB battery, with a $Ti_3C_2S_2$ MXene anode.

reported in Ref. [30] for the Li ion.

Despite the strong adsorption, there is a very low migration barrier (0.049 eV) which is much lower than the one calculated in the Li-case (0.29 eV [30]) for the same material. This fact indicates that the use of $Ti_3C_2S_2$ as anode electrode in MIB could potentially ensure faster charge/discharge rates than in the LIB case, as the Mg ion will be much more mobile than the Li ion. During charging of an Mg-ion battery cell, Mg ions leave the positive electrode (cathode) and move through the electrolyte to the negative electrode (anode). We have, therefore, a storage of energy to the anode. During discharging of the battery, this energy is released, and Mg ions move back to the cathode. A schematic of this working cycle, including the $Ti_3C_2S_2$ MXene anode, can be seen in Fig. 3.

This value of 0.049 eV is also comparable to the one for $Ti_3C_2Cl_2$–Li as reported by Papadopoulou et al. [30], which was equal to $E_{act} = 0.03$ eV, where E_{act} is the activation energy for diffusion, and was stated to be the lowest migration barrier so far when it comes to the use of $Ti_3C_2T_x$ as the basis material. A comparison of the migration barriers in both LIB and MIB can be seen in Fig. 4. Therefore, taking under consideration the many advantages of MIB over LIB as described in detail in Section I, $Ti_3C_2S_2$–Mg can be a safer, lower cost alternative to $Ti_3C_2Cl_2$–Li for anode electrode.

Regarding the transition state, the BVS model predicted the exact position of the TS Mg ion, which was on top of the S atom in the front view of the MXene layer, as shown in the right panels of Fig. 2. BVS completed the calculations in a small fraction of the time it took to run the CASTEP calculations. The BVS, however, resulted in a minimum pathway energy ($E_{BVS} = D_0 \left[\sum_{j=1}^{N_X} \frac{(s_{A-X_j} - s_{min})^2}{s_{min}^2} - N \right] + E_{rep}$ [38,40,46]; D_0 bond dissociation energy, N number of anions X the cation A bonds with, E_{rep} penalty term due to Coulomb repulsions, $s_{\min}$ valence corresponding to the equilibrium distance between A and X [47]) equal to 0.003 eV. This underestimation in activation energy in the BVS model has been previously reported not to affect the results when comparing two different structures [40], i.e., E_{BVS} keeps the trend in E_{act} between various materials intact. For a more in-depth analysis of the BVS model, one should refer to Ref. [32], as it is not under the scope of the present study.

As an outlook for the future research, the following study should be carried out: Zhu et al. [2], as mentioned in Section I, found migration barriers for an Mg ion equal to 0.57 eV and 0.53 eV when the interlayer spacing increased from 1.4 nm to 1.8 nm respectively. Such a behavior is consistent with the recent findings by Zhang et al. [48] who by means of molecular dynamics simulations on a layer by layer basis showed that the activation free energy gradient controls interfacial mobility in thin polymer films in a fashion similar to that predicted by a thermodynamical model (e.g. see Refs. [49–51]) stating that $g^f = cB\Omega$, where g^f is the activation free energy for diffusion, B stands for the isothermal bulk modulus, Ω the mean volume per atom and c is a constant practically independent of temperature and pressure. It is worthwhile to investigate whether such an interlayer spacing behavior also holds for the present case for Mg ion diffusion in the $Ti_3C_2S_2$ MXene.

4. Summary and concluding remarks

Performing electronic structure calculations within the framework of DFT, we obtained Ti_3C_2 MXene structure with S termination atoms. We found that the termination atoms sit in the fcc positions on the surface of the MXene.

In addition, a study of the adsorption energy for a single Mg ion on the surface of the $Ti_3C_2S_2$ MXene showed strong adsorption, in particular, − 1.75 eV. This value indicates that the Mg ion is more strongly bonded to the surface of the $Ti_3C_2S_2$ MXene than a Li ion on the same material (−1.52 eV [30]).

Furthermore, we calculated the energy barrier for diffusion of a Mg

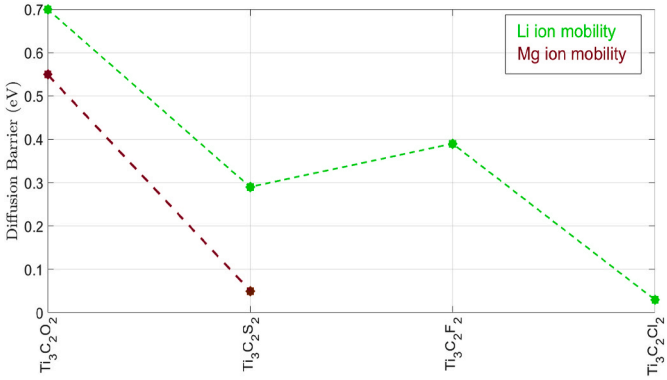

Fig. 4. The migration energy barriers for LIB and MIB using Ti_3C_2-based MXene anodes. The value for $Ti_3C_2O_2$–Mg was taken from Ref. [2].

ion on the surface of the $Ti_3C_2S_2$ MXene. We found a very low migration barrier (0.049 eV), the lowest one found so far for Mg in a $Ti_3C_2T_x$ structure and comparable to that found by Papadopoulou et al. [30] for a Li ion in the same structure which was equal to 0.03 eV. This fact can possibly ensure fast charge/discharge rate if we use $Ti_3C_2S_2$ as anode electrode in MIB.

The present theoretical study demonstrated the promise of Mg carriers in the $Ti_3C_2S_2$ MXene system and we anticipate that it will motivate further experimental studies in these systems for battery applications.

Author statement

Konstantina A. Papadopoulou: Conceptualization, Methodology, Validation, Formal Analysis, Investigation, Resources, Data Curation, Writing - Original Draft, Visualization, **Alexander Chroneos:** Conceptualization, Writing - Review & Editing, Project administration **Stavros-Richard G. Christopoulos:** Conceptualization, Methodology, Validation, Resources, Writing - Review & Editing, Supervision, Project administration, Funding acquisition.

Data availability

Data sharing is not applicable to this article as no new data were created or analyzed in this study.

Declaration of competing interest

The authors declare that they have no known competing financial interests or personal relationships that could have appeared to influence the work reported in this paper.

Acknowledgments

The authors acknowledge support from the International Consortium of Nanotechnologies (ICON) funded by Lloyd's Register Foundation, a charitable foundation which helps to protect life and property by supporting engineering-related education, public engagement and the application of research.

References

[1] M. Mirzaeian, Q. Abbas, M.R. Hunt, A. Galeyeva, R. Raza, Adv. Funct. Mater. 23 (2021) 947.
[2] J. Zhu, R. Shi, Y. Liu, Y. Zhu, J. Zhang, X. Hu, L. Li, Appl. Surf. Sci. 528 (2020), 146985.
[3] M. Li, J. Lu, Z. Chen, K. Amine, Adv. Mater. 30 (2018), 1800561.
[4] K.A. Papadopoulou, A. Chroneos, D. Parfitt, S.-R.G. Christopoulos, J. Appl. Phys. 128 (2020), 170902.
[5] B. Anasori, Y. Gogotsi, 2D Metal Carbides and Nitrides (MXenes), Springer, 2019.
[6] M.-Q. Zhao, C.E. Ren, M. Alhabeb, B. Anasori, M.W. Barsoum, Y. Gogotsi, ACS Appl. Energy Mater. 2 (2019) 1572.
[7] D. Aurbach, Z. Lu, A. Schechter, Y. Gofer, H. Gizbar, R. Turgeman, Y. Cohen, M. Moshkovich, E. Levi, Nature 407 (2000) 724.
[8] Z. Zhang, S. Dong, Z. Cui, A. Du, G. Li, G. Cui, Small Methods 2 (2018), 1800020.
[9] C. Eames, M.S. Islam, J. Am. Chem. Soc. 136 (2014) 16270.
[10] M. Naguib, M. Kurtoglu, V. Presser, J. Lu, J. Niu, M. Heon, L. Hultman, Y. Gogotsi, M.W. Barsoum, Adv. Mater. 23 (2011) 4248.
[11] M.W. Barsoum, T. El-Raghy, Am. Sci. 89 (2001) 334.
[12] Z. Sun, Int. Mater. Rev. 56 (2011) 143.
[13] M. Radovic, M.W. Barsoum, Am. Ceram. Soc. Bull. 92 (2013) 20.
[14] L. Verger, V. Natu, M. Carey, M.W. Barsoum, Trends Chem. 1 (7) (2019) 656–669.
[15] Y. Xie, Y. Dall'Agnese, M. Naguib, Y. Gogotsi, M.W. Barsoum, H.L. Zhuang, P. R. Kent, ACS Nano 8 (2014) 9606.
[16] Y. Xie, M. Naguib, V.N. Mochalin, M.W. Barsoum, Y. Gogotsi, X. Yu, K.-W. Nam, X.-Q. Yang, A.I. Kolesnikov, P.R. Kent, J. Am. Chem. Soc. 136 (2014) 6385.
[17] M. Xu, S. Lei, J. Qi, Q. Dou, L. Liu, Y. Lu, Q. Huang, S. Shi, X. Yan, ACS Nano 12 (2018) 3733.
[18] H. Kaland, J. Hadler-Jacobsen, F.H. Fagerli, N.P. Wagner, Z. Wang, S.M. Selbach, F. Vullum-Bruer, K. Wiik, S.K. Schnell, Sustain. Energy Fuels 4 (2020) 2956.
[19] G. Chaney, D. Cakir, F.M. Peeters, C. Ataca, Phys. Chem. Chem. Phys. 23 (44) (2021) 25424–25433.
[20] J. Zhu, A. Chroneos, U. Schwingenschlögl, Phys. Status Solidi Rapid Res. Lett. 9 (2015) 726.
[21] C.J. Zhang, S. Pinilla, N. McEvoy, C.P. Cullen, B. Anasori, E. Long, S.-H. Park, A. Seral-Ascaso, A. Shmeliov, D. Krishnan, et al., Chem. Mater. 29 (2017) 4848.
[22] A. Jain, S.P. Ong, G. Hautier, W. Chen, W.D. Richards, S. Dacek, S. Cholia, D. Gunter, D. Skinner, G. Ceder, Apl. Mater. 1 (2013), 011002.
[23] S.J. Clark, M.D. Segall, C.J. Pickard, P.J. Hasnip, M.I. Probert, K. Refson, M. C. Payne, Z. für Kristallogr. - Cryst. Mater. 220 (2005) 567.
[24] P. Hohenberg, W. Kohn, Phys. Rev. 136 (1964) B864.
[25] W. Kohn, L.J. Sham, Phys. Rev. 140 (1965) A1133.
[26] M.C. Payne, M.P. Teter, D.C. Allan, T. Arias, J.D. Joannopoulos, Rev. Mod. Phys. 64 (1992) 1045.
[27] B.G. Pfrommer, M. Cote, S.G. Louie, M.L. Cohen, J. Comput. Phys. 131 (1997) 233.
[28] D. Vanderbilt, Phys. Rev. B 41 (1990) 7892.
[29] W. Wan, H. Wang, Materials 8 (2015) 6163.
[30] K.A. Papadopoulou, D. Parfitt, A. Chroneos, S.-R.G. Christopoulos, J. Appl. Phys. 130 (2021), 095101.
[31] D. Packwood, J. Kermode, L. Mones, N. Bernstein, J. Woolley, N. Gould, C. Ortner, G. Csányi, J. Chem. Phys. 144 (2016), 164109.
[32] I.D. Brown, Chem. Rev. 109 (2009) 6858.
[33] N. Govind, M. Petersen, G. Fitzgerald, D. King-Smith, J. Andzelm, Comput. Mater. Sci. 28 (2003) 250.
[34] M. Avdeev, M. Sale, S. Adams, R.P. Rao, Solid State Ionics 225 (2012) 43.
[35] I.D. Brown, Bond Valences (2013) 11–58.
[36] J. Gao, G. Chu, M. He, S. Zhang, R. Xiao, H. Li, L. Chen, Sci. China Phys. Mech. Astron. 57 (2014) 1526.
[37] R. Xiao, H. Li, L. Chen, Sci. Rep. 5 (2015) 1.
[38] B. He, S. Chi, A. Ye, P. Mi, L. Zhang, B. Pu, Z. Zou, Y. Ran, Q. Zhao, D. Wang, et al., Sci. Data 7 (2020) 1.
[39] L. Pauling, J. Am. Chem. Soc. 51 (1929) 1010.
[40] K.A. Papadopoulou, A. Chroneos, S.-R.G. Christopoulos, Comput. Mater. Sci. 201 (2022), 110868.
[41] H. Chen, L.L. Wong, S. Adams, Acta Crystallogr. B: Struct. Sci. Crystal Eng. Mater. 75 (2019) 18.
[42] H. Chen, S. Adams, IUCrJ 4 (2017) 614.
[43] K. Momma, F. Izumi, J. Appl. Crystallogr. 44 (2011) 1272.
[44] Z.W. Seh, K.D. Fredrickson, B. Anasori, J. Kibsgaard, A.L. Strickler, M. R. Lukatskaya, Y. Gogotsi, T.F. Jaramillo, A. Vojvodic, ACS Energy Lett. 1 (2016) 589.
[45] C. Zhan, W. Sun, Y. Xie, D.-e. Jiang, P.R. Kent, ACS Appl. Mater. Interfaces 11 (2019) 24885.
[46] L.L. Wong, K.C. Phuah, R. Dai, H. Chen, W.S. Chew, S. Adams, Chem. Mater. 33 (2021) 625.
[47] S. Adams, Bond Valences (2013) 91–128.
[48] W. Zhang, F.W. Starr, J.F. Douglas, J. Chem. Phys. 155 (2021), 174901.
[49] K. Alexopoulos, P. Varotsos, Phys. Rev. B 24 (1981) 3606.
[50] P. Varotsos, K. Alexopoulos, Phys. Rev. B 22 (1980) 3130.
[51] P. Varotsos, K. Alexopoulos, Phys. Rev. B 24 (1981) 904.